MICROWAVE REFLECTION, DIFFRACTION AND TRANSMISSION STUDIES OF MAN

NAVAL AEROSPACE MEDICAL RESEARCH LABORATORY

7 FEBRUARY 1974

Unclassified
Security Classification

AD- 780226

DOCUMENT CONTROL DATA - R & D

Security classification of title, body of abstract and indexing annotation must be entered when the overall report is classified)

1. ORIGINATING ACTIVITY (Corporate author)

Naval Aerospace Medical Research Laboratory
Pensacola, Florida 32512

2a. REPORT SECURITY CLASSIFICATION

Unclassified

2b. GROUP

N/A

3. REPORT TITLE

Microwave Reflection, Diffraction and Transmission Studies of Man

4. DESCRIPTIVE NOTES (Type of report and inclusive dates)

N/A

5. AUTHOR(S) (First name, middle initial, last name)

Vernon R. Reno

6. REPORT DATE	7a. TOTAL NO. OF PAGES	7b. NO. OF REFS
7 February 1974	46	15

8a. CONTRACT OR GRANT NO	9a. ORIGINATOR'S REPORT NUMBER(S)
b. PROJECT NO DuMed MF51.524.015-0012BE7X	NAMRL-1199
c.	9b. OTHER REPORT NO(S) (Any other numbers that may be assigned this report)
d.	.2

10. DISTRIBUTION STATEMENT

Approved for public release; distribution unlimited.

11. SUPPLEMENTARY NOTES	12. SPONSORING MILITARY ACTIVITY
N/A	N/A

13. ABSTRACT

Basic, detailed information is not available concerning the changes in energy distribution in a microwave field caused by the introduction of man or animals. For safety monitoring, power measurements in proximity to man may be subject to gross errors in interpretation if these changes are not taken into consideration. Similar errors could result if the field perturbations caused by other nearby personnel or reflecting objects are not recognized.

A systematic, detailed description of the spatial energy distribution in microwave fields in proximity to man is provided for the first time. Graphic information is provided to demonstrate the effects on the energy distribution of different radiation parameters such as frequency and polarization and of the ratio of subject size to wavelength. The field patterns obtained with man are compared to theoretical studies of simpler objects available in the literature.

The information obtained in the present studies is immediately applicable to hazard evaluations and to the design of bioeffect investigations. The most significant benefit of the approach is in the potential for development of a new, noninvasive method for estimating the energy absorbed by man or animals from an incident microwave field.

DD FORM 1 NOV 65 1473

S/N 0102-014-6600

Unclassified
Security Classification

14 KEY WORDS	LINK A		LINK B		LINK C	
	ROLE	WT	ROLE	WT	ROLE	WT
Nonionizing radiation						
Microwave						
Biological effects						
Energy distribution						
Energy absorption						
Field patterns						
Reflection						
Diffraction						
Transmission						
Scattering						
Low intensity fields						
Man						

Approved for public release; distribution unlimited.

MICROWAVE REFLECTION, DIFFRACTION AND TRANSMISSION STUDIES OF MAN

Vernon R. Reno

Bureau of Medicine and Surgery
MF51.524.015-0012BE7X

Approved by

Ashton Graybiel, M. D.
Assistant for Scientific Programs

Released by

Captain N. W. Allebach, MC USN
Officer in Charge

7 February 1974

Naval Aerospace Medical Research Laboratory
Naval Aerospace Medical Institute
Naval Aerospace and Regional Medical Center
Pensacola, Florida 32512

SUMMARY PAGE

THE PROBLEM

The introduction of living organisms, including man, into a microwave field causes pronounced changes in the energy distribution in that field. The significance of these changes must be recognized in the interpretation of field intensity measurements made for exposure estimations, in experimentation designed to detect the bioeffects of non-ionizing radiation, and in hazard evaluations. Basic, detailed information concerning the characteristics and extent of these field perturbations is not available, particularly in proximity to man.

A more difficult problem exists in estimating the energy absorbed by man from an incident microwave field. A satisfactory theoretical solution to this problem is contingent on the development of a model that incorporates all of the significant parameters in the proper relationship to each other. In view of the extreme complexity of man, development of such a model is a formidable task. Once the task is accomplished, validation of the model remains a problem.

A unique approach to these problems is in progress at this laboratory as a part of a more comprehensive investigation of the effects of low intensity microwave radiation on man and animals. The approach is based on the direct measurement of the microwave energy reflected, diffracted and transmitted by man. It automatically takes into account the complex nature of the living subject and thereby minimizes the need for extrapolations from either living or nonliving models.

FINDINGS

A systematic, detailed description of the spatial energy distribution in microwave fields in proximity to man is given for the first time. Graphic information is provided to demonstrate the effects on the energy distribution of the relationships between the subject and different parameters of the radiation such as frequency and polarization. Selected inanimate objects were used in the same measurement framework to identify specific components of the diffraction patterns and to provide a connecting link through which the information gained with man can be related to more extensive studies of simpler objects reported in the literature. Characteristics of the diffraction patterns are identified which indicate the absorption of the incident energy by man.

The information obtained in the present studies is immediately applicable to the design of bioeffect investigations and to hazard evaluations. The most significant benefit of the approach, however, is in the potential for development of a new, noninvasive method for estimating the energy absorbed by man from a microwave field. The results of the present investigation provide basic information that is prerequisite to the development of such a method.

ACKNOWLEDGMENTS

This report is part of a study on the "Effects of microwave radiation on man" with Dietrich E. Beischer, Ph.D. as principal investigator.

Appreciation is extended to Messrs. T. A. Griner and G. D. Prettyman for assistance in making the measurements and to Messrs. I. W. Fuller, Jr. and T. A. Griner for participation in theoretical discussions.

TABLE OF CONTENTS

INTRODUCTION

A recurring, fundamental problem associated with studies of the effects of microwave radiation on man or other biosystems is that of estimating the energy actually absorbed by the system from an incident radiation field. The significance of the problem has been recognized by many investigators and attempts have been made to develop solutions based on both practical and theoretical considerations (13).

An investigation is in progress at this laboratory to evaluate the effects of low intensity microwave radiation on man and animals. Energy absorption considerations are of particular significance because of the low radiation intensities in use and consequent subtle effects that are anticipated. Optimum results would be expected from measurements taken with very small sensors embedded in the different tissues of interest. A survey, then, of the microwave fields within different tissues and organs would provide direct information on the absorbed dose. Unfortunately, a sensor suitable for this purpose does not exist, nor does it appear likely that so invasive a procedure could be justified at present, at least not with man.

Many of the accepted concepts for quantifying the interaction between biological systems and nonionizing radiation are applicable only under idealized conditions (15). These concepts were developed primarily during theoretical studies based on mathematical models intended to represent the living systems under consideration. Typical assumptions made for computational simplicity during such studies were the following: (a) the illumination was a simple plane wave, (b) the biosystem model was composed of one or multiple layers of homogeneous material having electrical properties reported for skin, fat or muscle tissue, and (c) the tissue models were arranged in a series of planar slabs or concentric spheres of selected dimensions.

Although considerable improvements have been made in the theoretical approach, the extent of the disparity between conditions as they exist in reality and those assumed by some of the models can be appreciated by consideration of some significant factors relevant to the examples cited: (a) It is unlikely that a plane wave will be present at an area in which hazardous power levels are to be anticipated. In fact, because of multipath reflections, considerable effort is often required to obtain a plane wave even in an area located at a sufficient distance from the radiator to be in the far field. Plane wave considerations are not always appropriate in the near field of an antenna where power levels are highest (15). (b) The amount of energy deposited in a tissue immersed in a microwave field is critically dependent on its dielectric and loss properties, which could be expected to vary according to the type of tissue. In addition, any boundary between tissues of differing composition is capable of causing reflections, if the adjacent tissues differ in dielectric properties. The reflections from the boundaries can sum to form multiple foci of energy and localized "hot spots" throughout the tissue. Tang (12) and Adey (1) vividly demonstrated the complex nature of the microwave scattering obtained from dielectric-coated, conducting cylinders and solid, dielectric cylinders. Both studies show that the scattering properties of the objects vary widely, depending on both the type of dielectric and the relationship between the size and shape of the reflecting object and the wavelength of the radiation.

Complex scattering behavior was observed by these authors from objects of simple shape composed of a single homogeneous dielectric material or of a conductor covered by a single, homogeneous layer of dielectric. In both cases the reflecting objects were extremely simple and regular in shape and composition as compared to man and most other living organisms. Man, to the contrary, is neither homogeneous in composition nor simple in shape but is extremely complex from the microwave point of view. Man's tissues are generally stratified with multiple layers of materials of differing dielectric properties intermixed in different proportions according to the function of the tissue or organ. The resultant mixture should have dielectric properties that are different from those of any of its constituents (14). Additional changes in the mixture proportions, and therefore the dielectric properties, could be expected to follow dilation of the capillaries and perfusion of the tissues with blood--a normal dynamic change of considerable magnitude that occurs in response to a shift in the tissue from a resting to an active state (10). In addition to changing the dielectric properties, the increase in capillary flow changes the heat transfer characteristics of the tissue and, therefore, the ability to dissipate energy. The tissues, permeated to differing degrees by conductors in the form of blood and lymph, may be organized into either sheet-like structures of varying thickness and loss factors, or solid, hollow or fluid-filled organs that vary over a wide range in their orientation and in the ratio of their size to the wavelength of the radiation.

There is, therefore, sufficient reason to at least question the validity and applicability of conclusions drawn on the basis of some of the models. To compound the problem, no reasonable method exists to evaluate the degree of validity of the models.

To ameliorate the problem, a unique approach was developed utilizing man himself as the experimental subject. The objective is to determine those basic characteristics of the interaction of the field with man that may be significant to experimental design in future studies and, if possible, to provide the foundation for an improved, noninvasive method for estimating the energy actually absorbed by man from an incident microwave field.

RATIONALE

Direct measurement of the energy reflected, diffracted and transmitted by an object can provide information concerning the properties of that object (7). This concept should remain valid even if that object is man. Determinations of the electrical energy density in proximity to man provide this information as a function of the radiation and absorption parameters. Similar measurements taken in proximity to simpler objects exposed to the same field conditions permit evaluation of the results of the studies with man in relation to theoretical and experimental investigations of inanimate objects. Some of these results were reported previously (3,4,9).

The intent to reduce assumptions and extrapolations to a minimum is implicit in this approach. This is the fundamental reason for the choice of man as the experimental subject. The choice of man also makes it possible to automatically take into account in the proper perspective the complex shape and ratios of size of the man to wavelength as well as the static and dynamic nature of the dielectric composition of living, functioning

tissues. A judicious combination of instrumentation and experimental protocol provides the necessary data with minimum exposure of the subject. For example, all of the measurements described in the present study required a total exposure of approximately 3 hours to incident fields of approximately 40 microwatts/cm^2 (μW/cm^2) distributed over a period of several weeks.

EXPOSURE AND MEASUREMENT FACILITIES

The facility used in the present investigation, unique in many respects, was designed specifically to permit short- and long-term studies of the effects of low intensity microwave radiation on man and the acute and chronic effects of low- and high-intensity radiation on animals. Only the most significant features will be discussed at this time. A complete description will appear in a subsequent report.

Traveling-wave-tube amplifier (TWTA) chains, driven by either one or two microwave sweepers, provide continuous wave (cw), pulsed, or swept-frequency radiation between 1 and 12.4 gigahertz (GHz). The output is monitored by a thermoelectric power meter. An additional high-power magnetron source is also available at a frequency of 2.45 GHz. The broad range of wavelengths permits frequency-scaling experiments in which the significance of the ratio of wavelength to subject size can be studied. Either amplitude or frequency modulation is available and changes in frequency and power can be programmed as desired on an external curve-tracking programmer. Monochromatic radiation is assured by filtering during single-frequency operation and multifrequency operation is possible. Frequency is monitored continuously by a crystal-controlled counter.

A large parabolic reflector (4.8 m in diameter) collimates the beam (11) in the range used in the present series of experiments. The reflector is fed by rotatable horns that provide any desired linear field polarization between horizontal and vertical (Figure 1). Although a more uniform field distribution could be attained by using an offset feed (2,11), practical considerations dictated otherwise because a larger reflector and housing area would be required. The field distribution obtained with the more conventional feed design was adequate for the present studies and is shown in the plots of the reference fields that follow. The beam illuminates an experimental area behind an aperture in an absorber wall 5.6 m from the reflector. Some improvement in the field distribution in the experimental area was achieved by expanding the aperture from the original size of 2.5 m X 2.5 m to the existing width of 3.6 m and height of 3.0 m. The front absorber wall reduces reflections into the antenna that would tend to degrade the field. An absorber backpanel located 2.5 m behind the absorber wall delimits the experimental area and minimizes reflections into it. The front absorber wall, aperture and absorber backpanel are coaxial with, and normal to, the beam axis. This arrangement also provides shielded areas for instrumentation above, below, and at both sides of the experimental area. The experimental area itself is designed to permit continuous habitation by human subjects and includes detachable sanitary facilities. Figure 2 indicates the relationships of the major range components and defines the coordinate system in use.

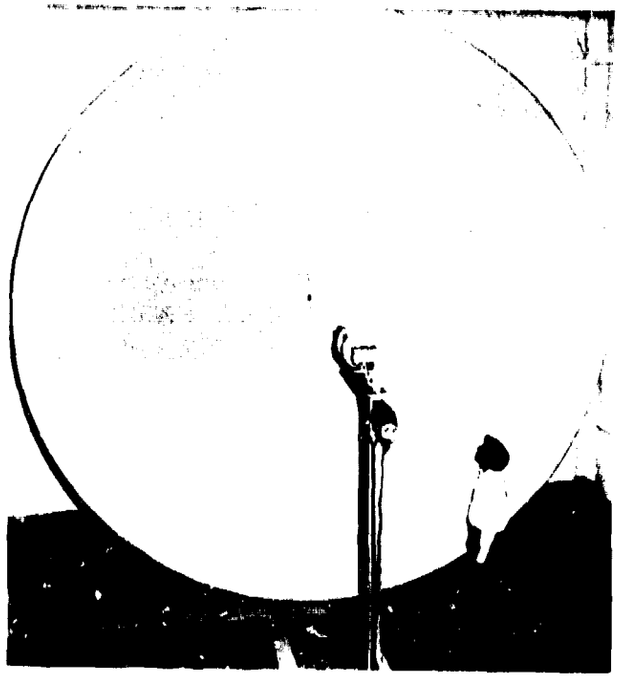

Figure 1

Parabolic Reflector and Feed

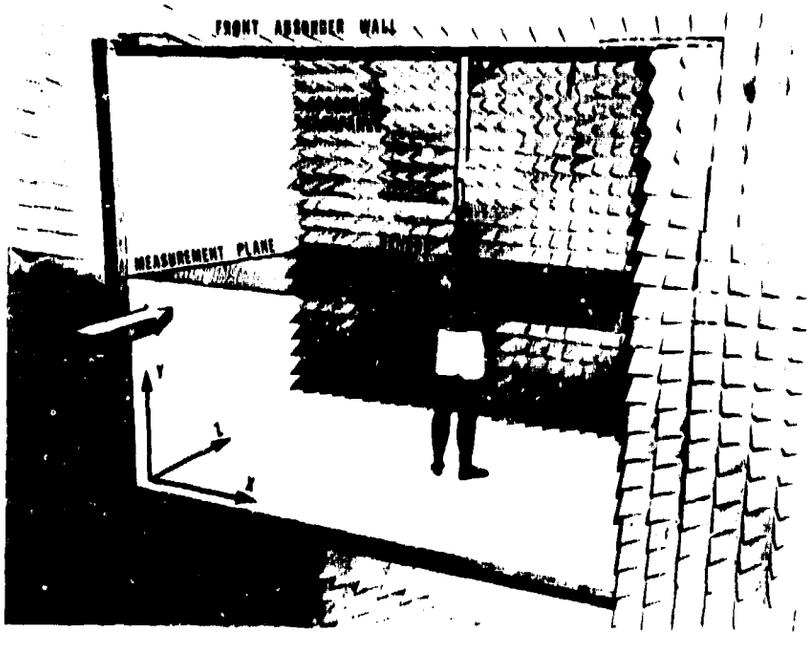

Figure 2

Experimental Area with Subject in Position for Measurements

Power measurements are based on recent concepts (15) and instrumentation developed, calibrated, and provided by the National Bureau of Standards. This instrumentation is an essential part of the total system. Three orthogonal dipoles were combined to form a very small isotropic sensor capable of measuring both near and far fields. In the configuration used in the present experiments the instrument provided a vector summation of the square of the electric vectors at a given point in space. Wacker and Bowman (15) gave a detailed theoretical discussion of the benefits of expressing the measurements in electrical energy density units. All energy density units in the present report can be multiplied by 60 to convert to the more familiar equivalent plane wave power density units ($\mu W/cm^2$). The high sensitivity of the instrument (0.3 nanojoules/cubic meter [nJ/m^3] full scale) permits accurate measurements at the low power levels used for human exposure, and the small size permits a high degree of spatial resolution with negligible perturbation of the field. The sensor of the instrument is mounted at the end of an arm suspended from an overhead gantry that drives in either of two orthogonal directions (X or Z). The sensor thus scans in a horizontal plane at an elevation selected by changing the length of the support arm (Figure 2). Since the support arm is also in the field and could affect the field, various materials and shielding arrangements for the arm were tested before the existing configuration was adopted. Analog voltages from the drive system indicate the spatial position of the sensor. A voltage from the power meter indicates the field intensity at the sensor position. The voltages are fed to either a minicomputer for further processing or directly to an X-Y recorder for plotting, or to both. Plots of the scans provide a systematic description of the spatial energy distribution throughout the experimental area.

PROCEDURE

The human subject or other object of interest was illuminated by horizontally or vertically polarized cw radiation at a frequency of either 1 or 3 GHz. Maximum intensity of the incident field at either frequency was approximately 0.7 nJ/m^3. A life-sized, fiberglas, male manikin, coated with two layers of silver conductive lacquer (Figure 3), was used in one series of measurements to simulate the size and shape of the human subject. Another series of measurements was based on a conducting, aluminum cylinder that had an adjustable diameter, a normally vertical axis, and ends that extended behind the upper and lower boundaries of the opening in the aperture wall. Successive scans of the field were made on all sides of the man or object at increasing distances on an X-Z plane. All measurements were taken on X-Z planes located either at the transparietal (head) or thoracic (chest) plane on the same human subject who was of normal size and physique. Preliminary measurements on other subjects provided similar results. Respiration was suspended and, in some cases, a custom-fitted, partial-body mold of styrofoam was used to prevent the subject's movement during the measurements at 3 GHz where motion-induced artifacts would be more significant due to the shorter wavelength.

The output power of the generator was held constant by continuous monitoring with a directional coupler and a digital, thermoelectric power meter. Since one of the objectives of the study was to determine the effects of frequency, it was imperative that

Figure 3

Life-sized Conductive Manikin Used to Simulate the Human Subject

monochromatic radiation be used to illuminate the subject. Therefore, a low-pass filter was used to remove harmonics and other spurious radiation from the signal fed to the antenna. Spectrum analysis of the signal demonstrated both the requirement for the filter and its efficacy (Figure 4).

Initial data processing was accomplished manually. Results of individual scans were traced from X-Y recorder plots, displaced on the X-axis and serially recombined to provide three-dimensional (3-D) views of the energy distribution patterns with and without the subject in the field. Contour plots of the same data were also prepared manually. Procedures were subsequently developed to process the data by minicomputer and output the results to an oscilloscope for observation and photographic registration. A combination of methods, dependent on the objective, is generally used. Examples of results obtained with the different methods are discussed in the next section.

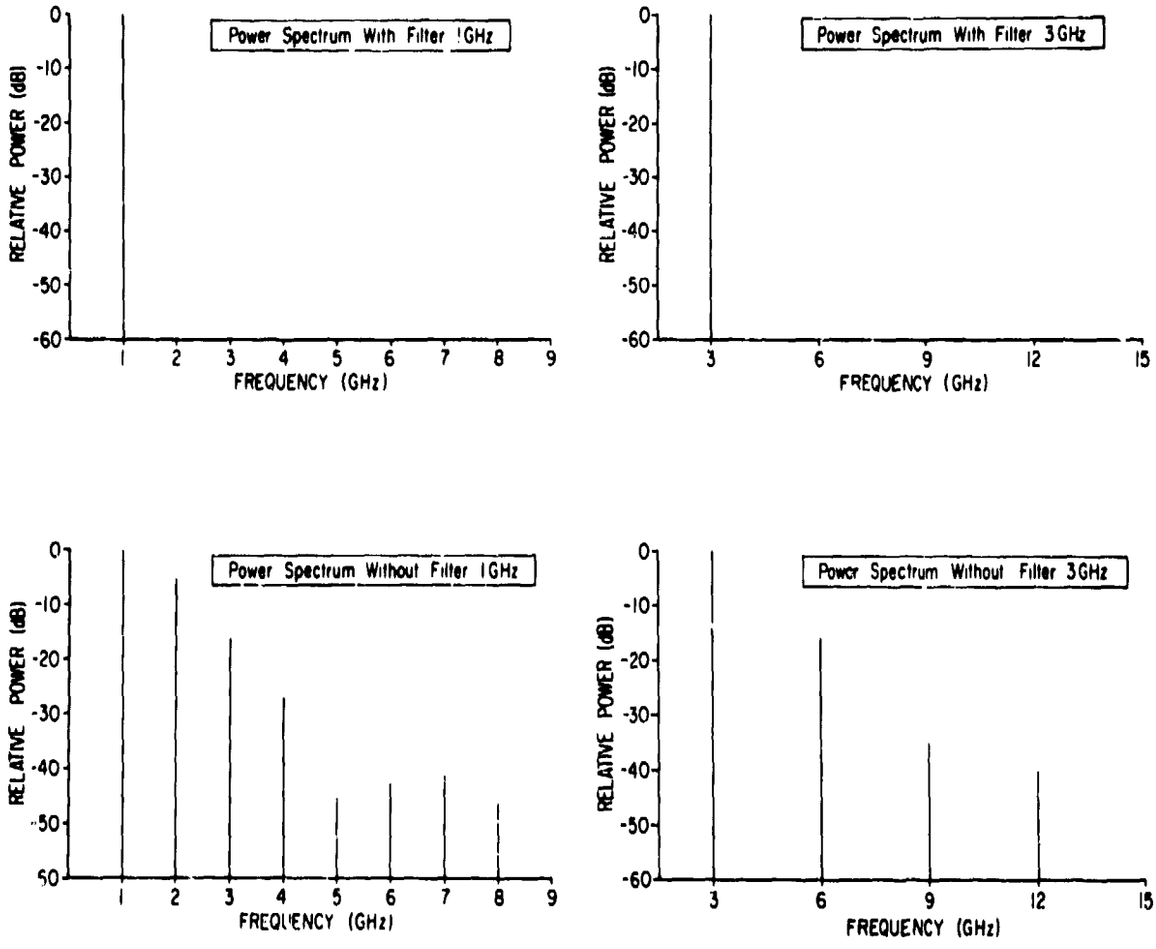

Figure 4

Power Spectrum of Radiation at 1 and 3 GHz With and Without Filters

RESULTS AND DISCUSSION

The spatial distribution of microwave energy in proximity to man or any other object is characteristic of the reflection, diffraction and transmission of that energy by the object. The effects of man on spatial distribution can be studied by comparison of the patterns of electrical energy distribution in unperturbed fields in the absence of the man with those following his introduction into the field. Information concerning the energy absorbed by the man is also contained in the same distribution patterns. Although the externally reflected and diffracted fields are of considerable interest in themselves, their relationship to the absorbed energy is more significant in considerations of dosimetry. Systematic microwave reflection and diffraction measurements in proximity to man have not been described previously or used in the context of experimental design of bioeffect studies or biological dosimetry.

The distribution of energy in the vicinity of man is dependent on other factors in addition to the energy actually absorbed. Among the most important of these other factors are: (a) the amplitude distribution of the field incident on the illuminated surface; (b) the frequency and polarization of the radiation; and (c) the size, shape, and dielectric composition of the man. The same fundamental considerations apply to any biosystem or object. An understanding of the theoretical and practical relationships among these factors, as expressed in the energy distribution patterns, is prerequisite to the proper design of bioeffects studies and to an estimation of absorption from the patterns.

The isotropic sensor used in the present studies actually measured the resultant of these parameters and was unable to discriminate in favor of the individual components. It is necessary, therefore, to identify the contribution of each component to the patterns and to evaluate its significance in terms of absorption. To assist in the evaluations, field observations were made in proximity to inanimate objects that are simpler than man in shape and electrical properties. The use of simpler objects in the same measurement framework should make it possible to relate the data taken with man to more comprehensive theoretical and experimental studies of simpler objects reported in the literature. For instance, King and Wu (8) described the reflection and diffraction of electromagnetic waves by conducting and dielectric objects of various shapes and size-to-wavelength ratios.

REFERENCE FIELD

The characteristics of the field incident on the subject influence the interpretation of the results of the pattern measurements. Considerable effort was made to optimize these characteristics within the constraints imposed by economic considerations and by the fact that these were real rather than idealized fields. The field distribution at the subject's location is primarily dependent on (a) the output of the generator and (b) the spatial distribution of the energy from the generator as determined by the antenna, feed arrangements, and any undesirable multipath reflections that may be present.

Figure 4 shows the results of the spectrum analysis of the output from the generator and the relative power at different frequencies with and without the filter. The generating system was operated at the same power level used during the reflection and diffraction studies, and the power levels of the respective fundamentals (1 and 3 GHz) were normalized to zero db to provide a base for comparison. Considerable energy is present at undesired frequencies if the filters are not used. This energy could result in erroneous conclusions if it were not accounted for in biological investigations--a point often neglected in previous biological studies. The distribution of energy across the band is dependent on the characteristics of the generator and should be investigated for each microwave exposure system.

The spatial distribution of the fields throughout the experimental area (Figures 5 through 7) shows that the structure of the field is related to the frequency and polarization of the radiation and to the plane of measurement. The data from these measurements were also grouped for manually constructed contour plots so that the fine structure was smoothed

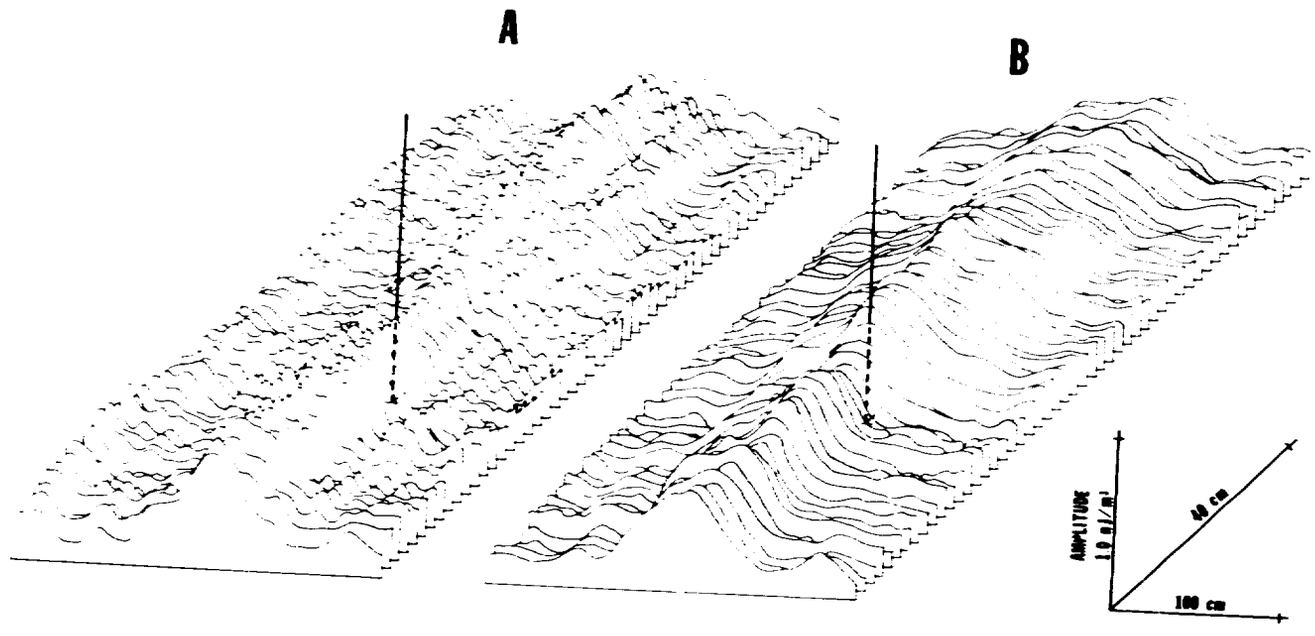

Figure 5

Energy Distribution in the Reference Field at 1 GHz at the Chest Plane. 3-D Presentation:

A. Vertical B. Horizontal

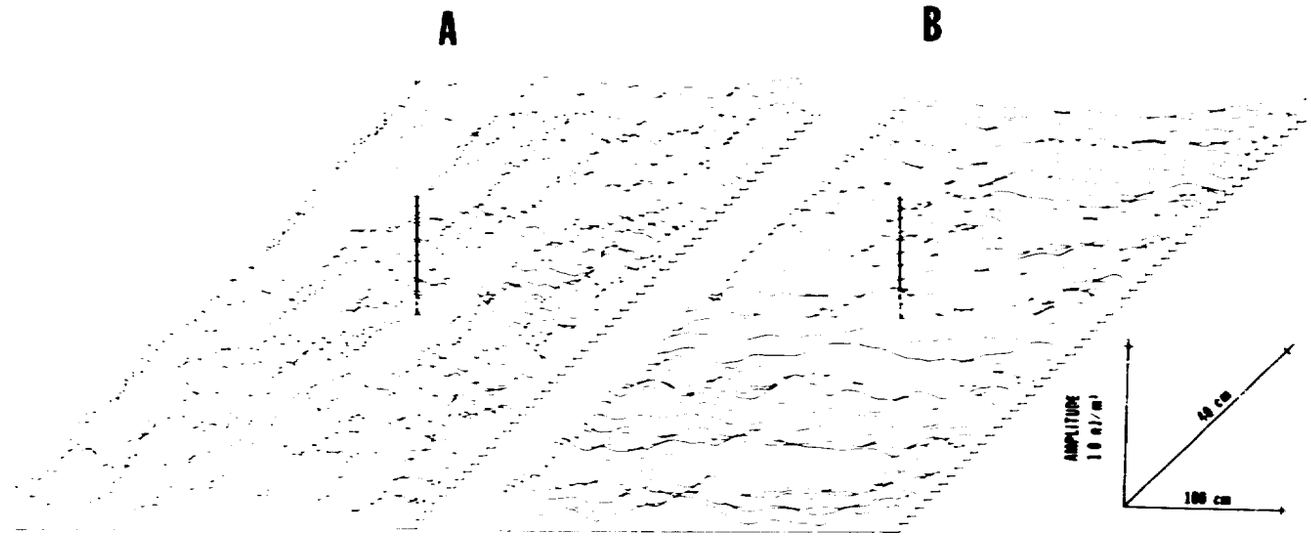

Figure 6

Energy Distribution in the Reference Field at 1 GHz at the Head Plane. 3-D Presentation:

A. Vertical B. Horizontal

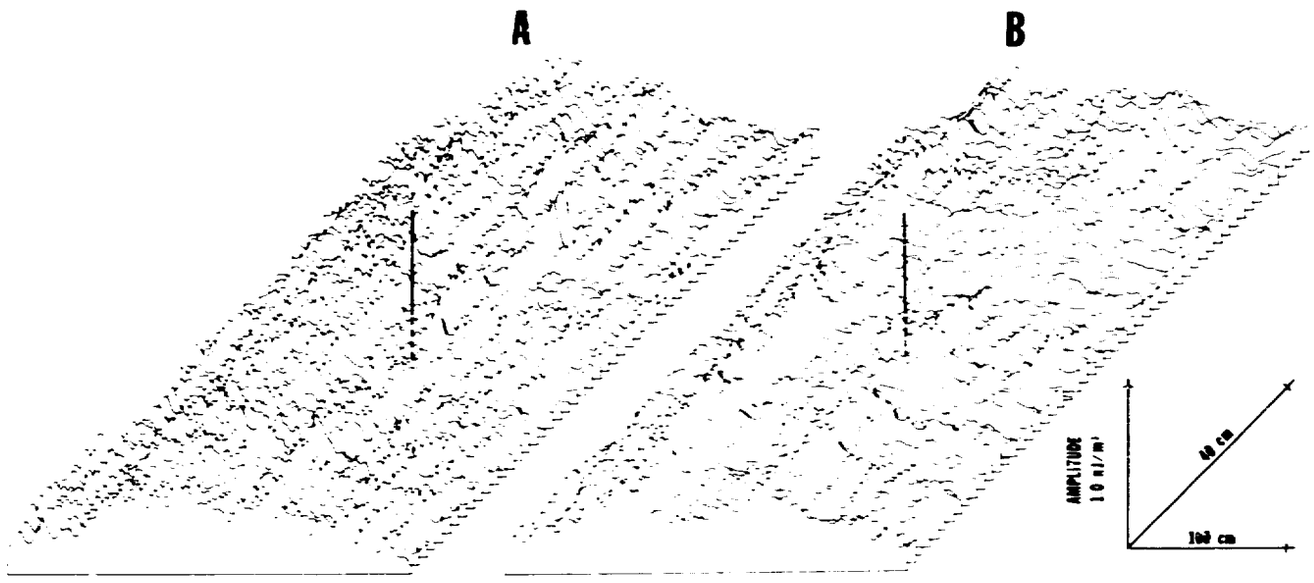

Figure 7

Energy Distribution in the Reference Field at 3 GHz at the Head Plane. 3-D Presentation:

A. Vertical B. Horizontal

and a semi-quantitative overview of the field was obtained. Contour plots of the reference fields at 1 GHz for vertical and horizontal polarization are shown in Figure 8. The energy incident on objects immersed in these fields would differ dependent on their location (Figures 5 through 8). Effects of these differences were reduced to a practical minimum by careful positioning of the subjects or objects at the same location in the field throughout the measurements. A vertical line in the field plots indicates the position of the center of the surface of the test objects proximal to the antenna. A reference-field plot was made for each permutation of radiation parameters to further reduce the possibility of error. Under idealized conditions, considerations of this type would not exist; however, they are typical of situations encountered in real fields.

ENERGY DISTRIBUTION IN PROXIMITY TO TEST OBJECTS

Introduction of the test object, including man, into the reference field caused the generation of pronounced perturbations and a standing-wave pattern of energy distribution which extended a considerable distance from the object. The characteristics of this new pattern are directly related to the frequency and polarization of the radiation and to the geometry and electrical properties of the test object. Consideration of these patterns will progress from those found in proximity to the simplest of the test objects used--the conducting cylinder--to the most complex--man.

Cylinder

The energy distribution at 1 GHz around a conducting cylinder is shown as a function of polarization in Figures 9 and 10. The cylinder diameter was set equal to the wavelength, and the measurement plane was established at chest height. The significance of the ratio of wavelength to cylinder diameter will be discussed later. Discontinuity in the data and the blank areas contiguous to the cylinder indicate the limits of measurement caused when the cylinder blocked the sensor scan. Irradiation of the cylinder produced the expected standing waves on the illuminated (proximal) side and shadow on the opposite side. The resultant diffraction field has a parabolic pattern with ridges of elevated energy extending well beyond the cylinder. The parabolic pattern of the energy distribution is particularly evident in Figure 10 A. Effects of polarization are clearly seen. If the electric field (E-field) is parallel to the axis of the cylinder (vertical polarization), the side structure of the field is more pronounced and of higher amplitude (Figure 9A); if the E-field is perpendicular to the axis (horizontal polarization), the energy in the side structure is considerably reduced although it is not zero (Figure 9B). Comparison of the field patterns in the vicinity of the cylinder with the respective reference fields (Figures 5 through 8) indicates the radical changes in energy distribution caused by the cylinder.

Theoretical and experimental treatments of the field distribution around conducting cylinders are available in the literature. Some of the information from a theoretical treatment by King and Wu (8) is redrawn in Figure 11 to indicate the calculated field distribution in the vicinity of a conducting cylinder illuminated by a plane wave. The radiation was so polarized that the E-field was parallel to the axis of the cylinder, and the cylinder diameter was equal to the wavelength. On the illuminated side of the cylinder a radial, standing-wave pattern is formed that diminishes in amplitude with increasing

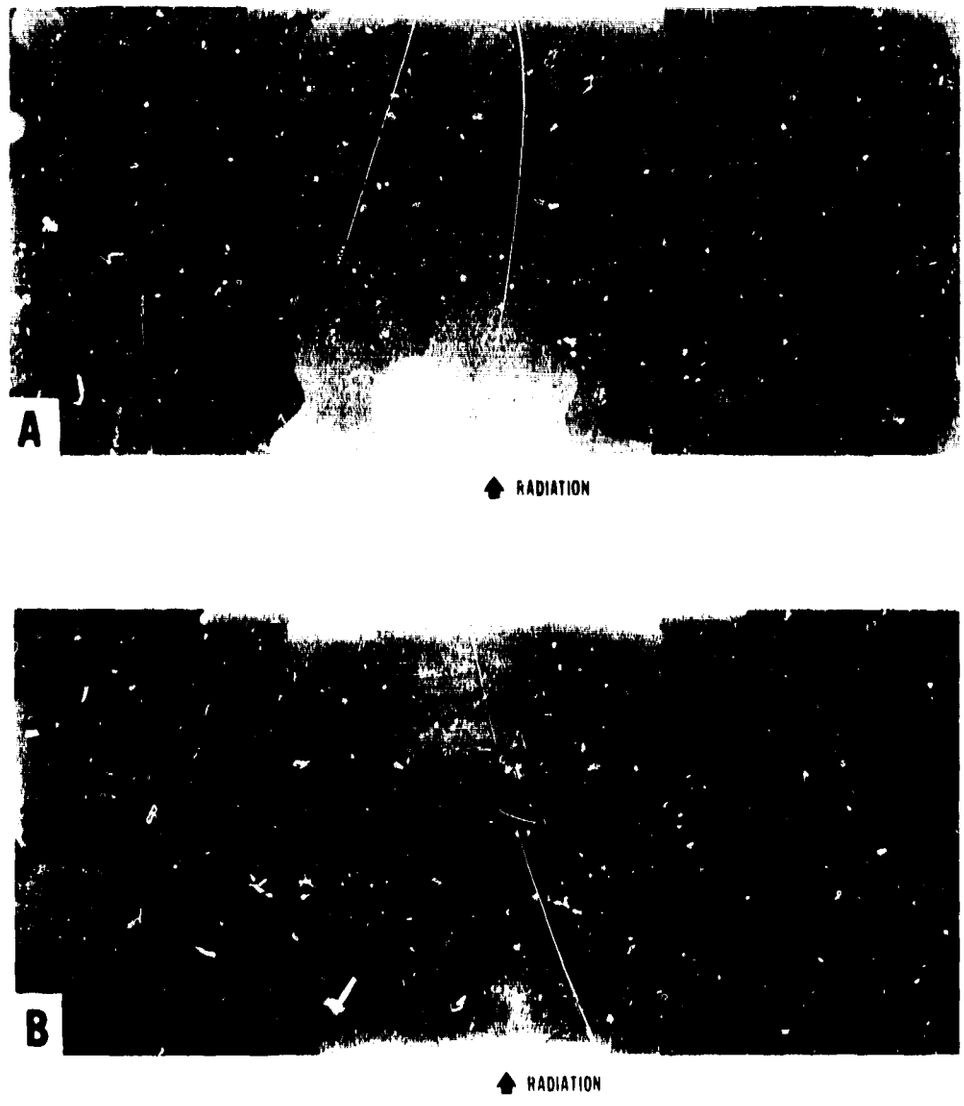

Figure 8

Energy Distribution in the Reference Field at 1 GHz at the Chest Plane

Contour Presentation: A. Vertical B. Horizontal

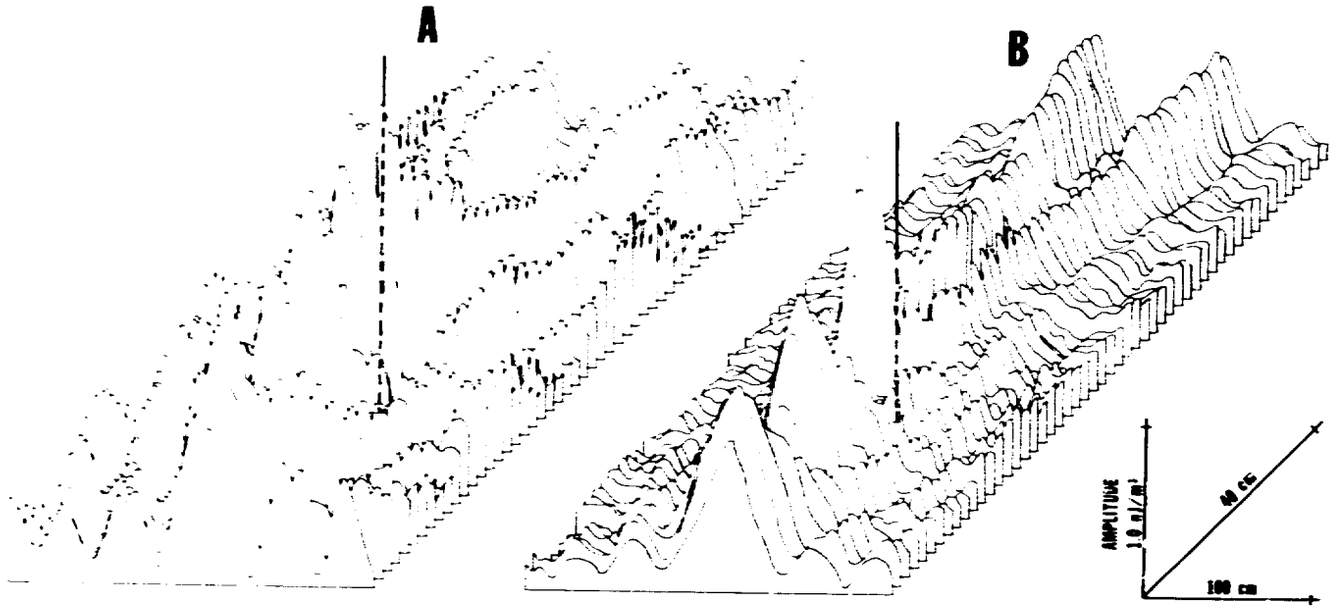

Figure 9

Energy Distribution in Proximity to the Conducting Cylinder at 1 GHz at the Chest Plane. 3-D Presentation:

A. Vertical B. Horizontal

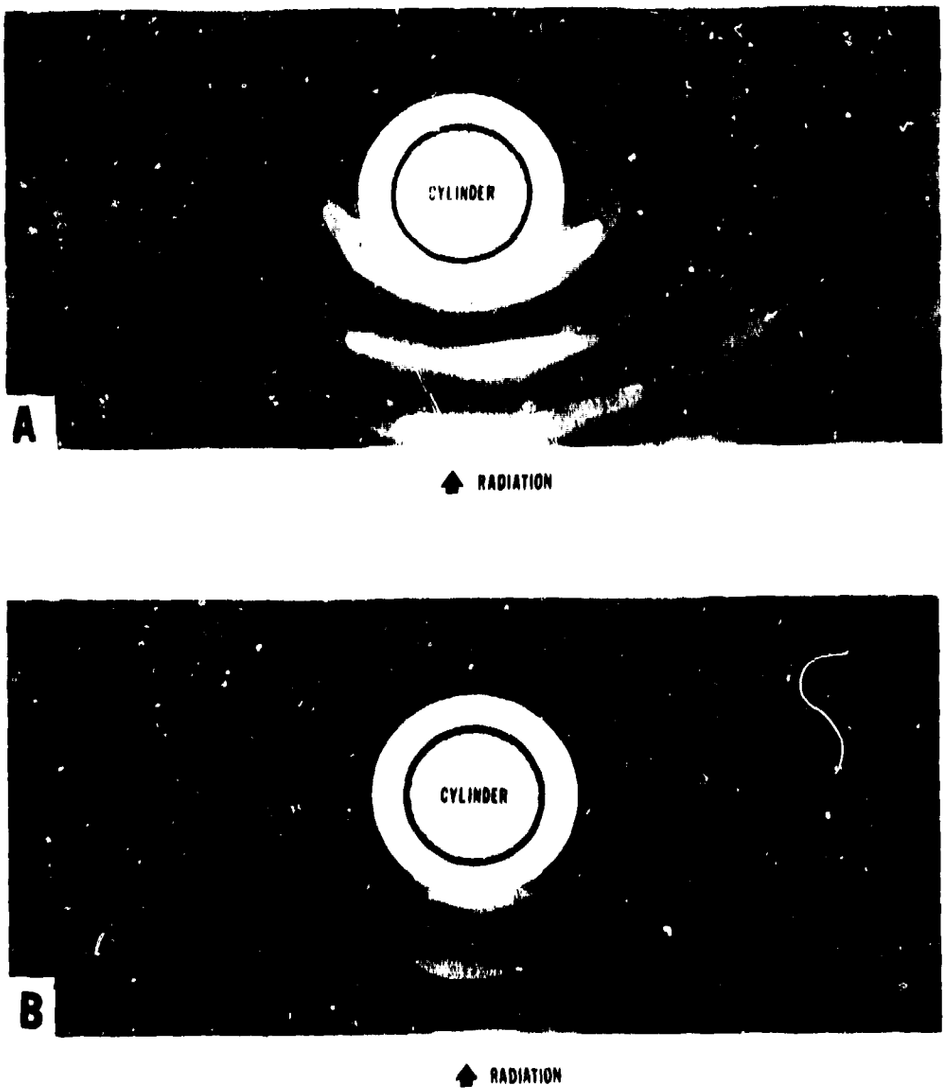

Figure 10

Energy Distribution in Proximity to the Conducting Cylinder at 1 GHz at the Chest Plane

Contour Presentation: A. Vertical B. Horizontal

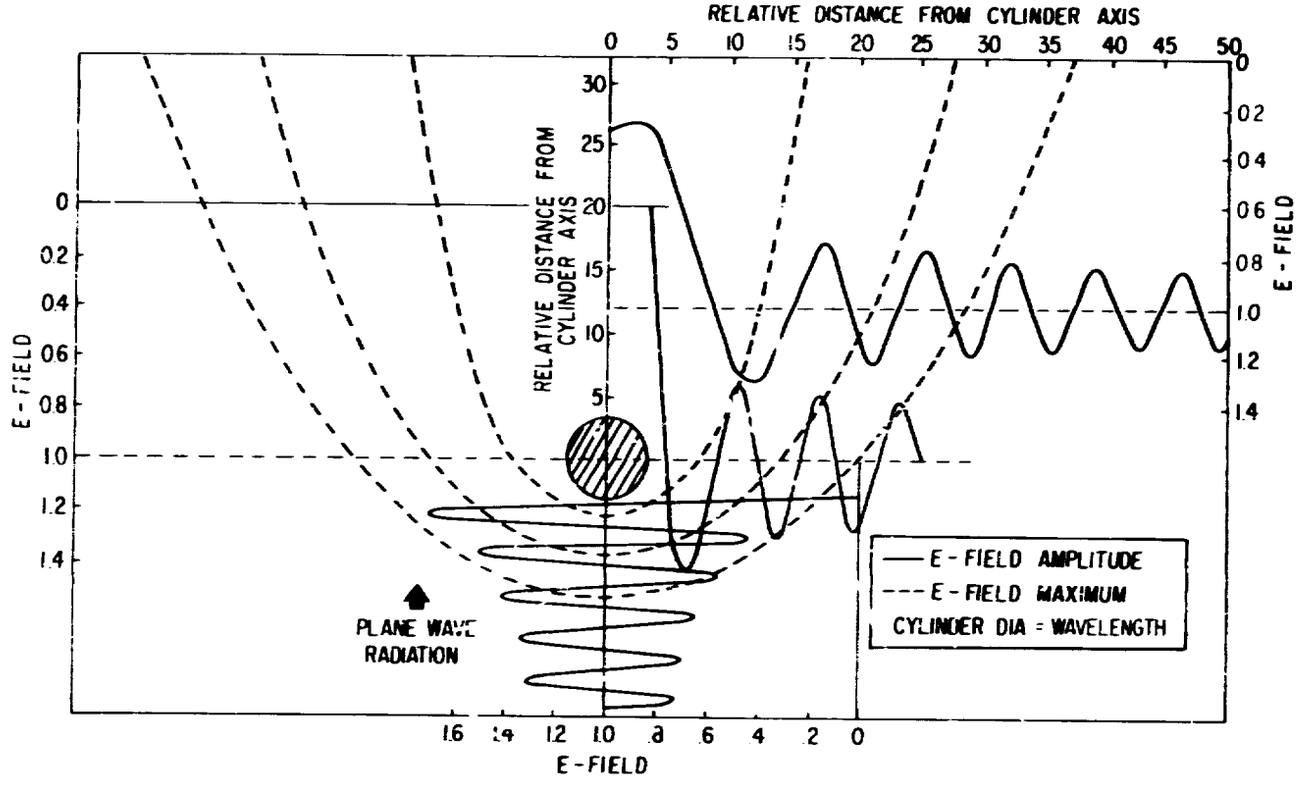

Figure 11

Theoretical Electrical Energy Distribution in Proximity to a Conducting Cylinder Illuminated by a Vertically Polarized Plane Wave (redrawn from King and Wu [8])

distance from the cylinder. A given maximum or minimum in the E-field advances outward from the cylinder along a parabolic path. King and Wu also show data experimentally determined by other investigators to indicate the excellent correlation between measured and calculated values.

The agreement between the field patterns measured in the present study and those reported in the literature can be appreciated by comparison of Figure 11 with A in both Figures 9 and 10. This comparison is significant in several respects. One of the problems associated with the experimental determination of the effect of object shape on microwave reflection is the calibration of the system. In radar investigations the standard procedure is to relate the scattering properties of the object of interest to those of some known object. This requires a standard reflector of simple geometry, such as a sphere or flat plate, for which the theoretical solution is known (5). In the present study the cylinder provides the calibration device as well as an intermediate link for relating measurements in proximity to more complex objects, such as man, to reported theoretical and experimental measurements near simpler objects.

Manikin

As indicated previously, the spatial distribution of electromagnetic fields in the vicinity of man is related to his geometry as well as to the electrical properties of his tissues. A series of experiments was designed to identify the influence of each of these factors on the field patterns so that they could be evaluated separately. For this purpose the life-sized manikin was used to simulate the geometry of the human subject. It was made conductive to provide nearly total reflection of the incident field and to exclude the influence of internal reflections (such as those that could be caused by differences in tissue properties in man), thereby limiting the field characteristics to those primarily due to the geometry of the object. The energy distribution in proximity to the manikin under different conditions is shown in Figures 12 through 17.

Chest Plane, 1 GHz. A 3-D display of the field at the chest plane at 1 GHz is shown as a function of polarization in Figure 12; Figure 13 consists of manually constructed contour curves, or top views of the field, based on the same data. The standing waves on the illuminated side of the manikin, the shadowed area on the opposite side, and the parabolic nature of the field are clearly evident. The structure of the fields is dependent on the polarization of the incident wave. The amplitude of the field structure at the sides of the peaks and shadow is reduced where the polarization is horizontal. However, the peak adjacent to the manikin and the trailing ends of the first intensity ridge are noticeably higher in amplitude. A difference in the shadow characteristics is evident in the contour plots (Figure 13). The shadow is narrow in the case of horizontal polarization but broadens with distance from the manikin when the polarization is vertical. Comparison of the diffraction fields around the manikin (Figures 12 and 13) with those in the vicinity of the cylinder (Figures 9 and 10) indicates differences in the peak formations and in the intensity ridges delimiting the shadow region.

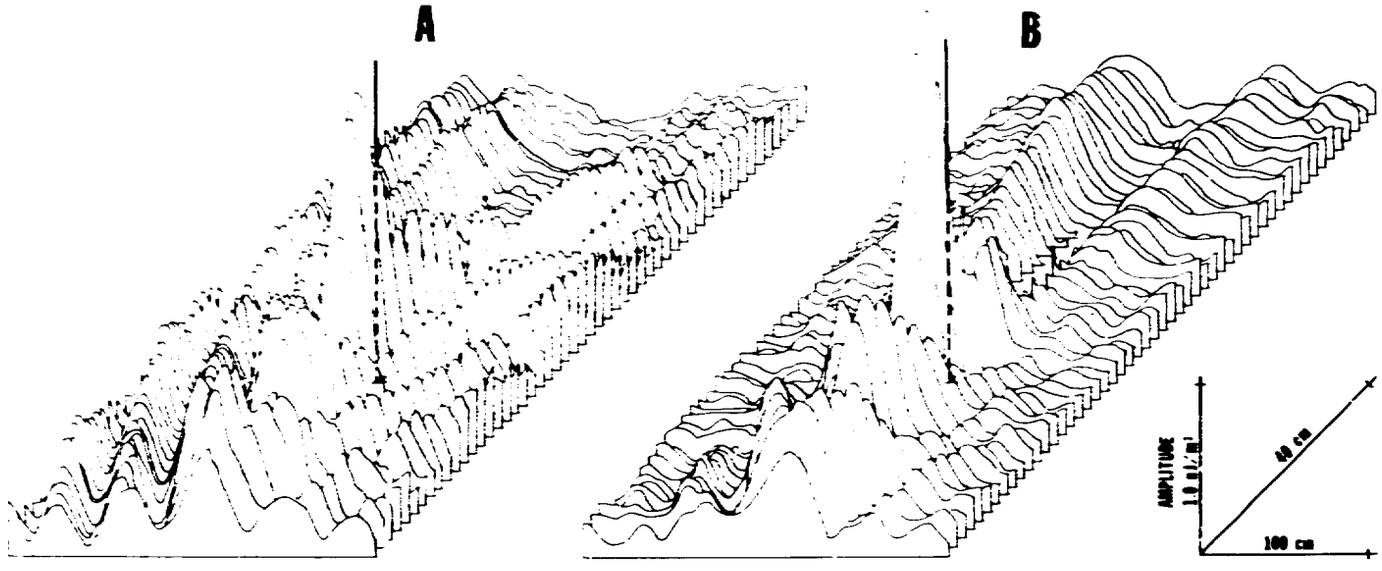

Figure 12

Energy Distribution in Proximity to the Conducting Manikin at 1 GHz at the Chest Plane. 3-D Presentation:

A. Vertical B. Horizontal

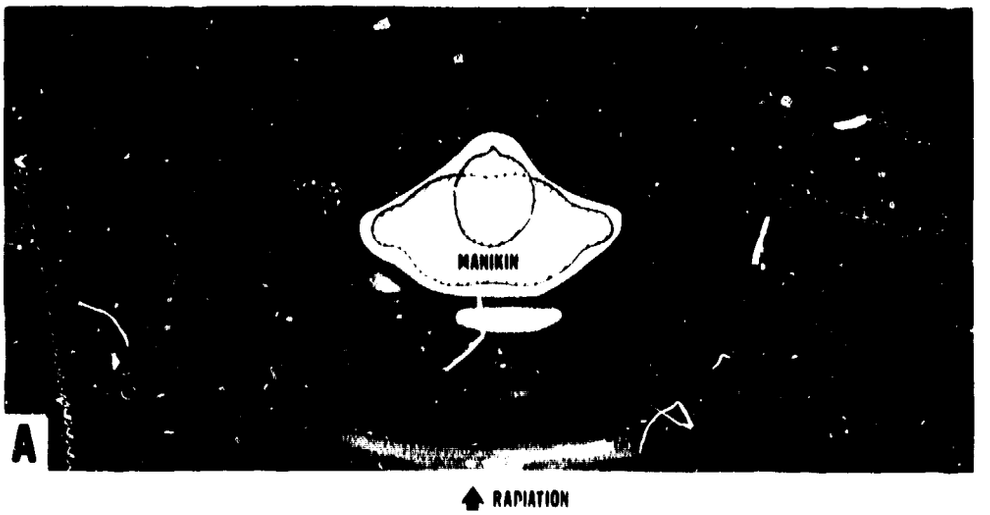

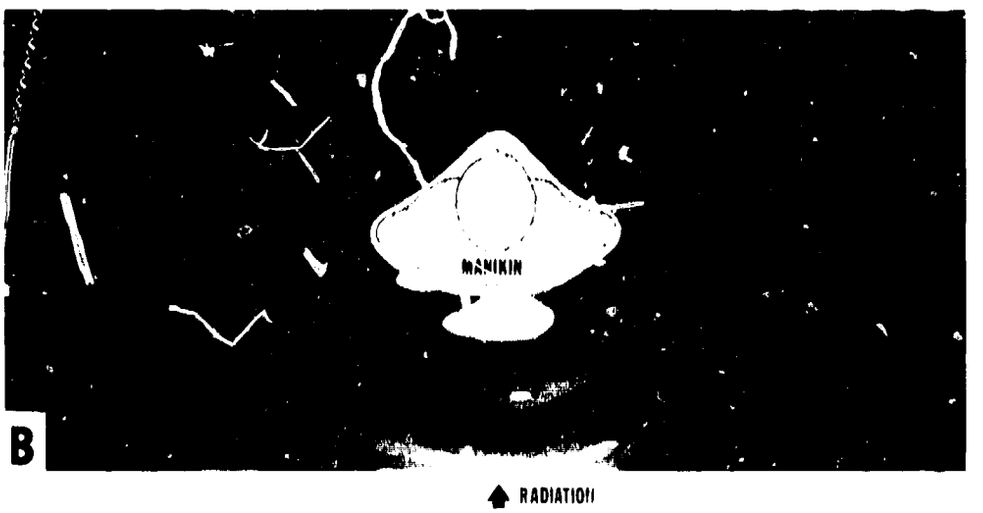

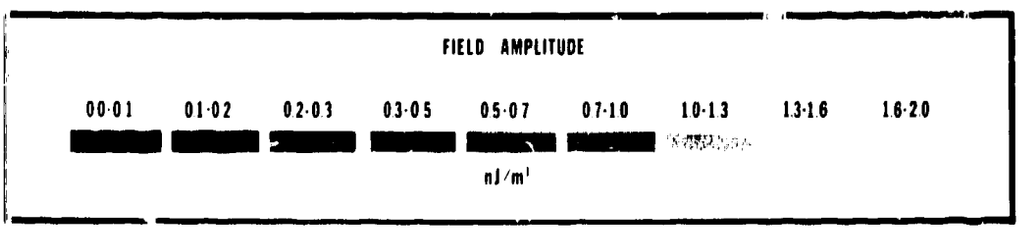

Figure 13

Energy Distribution in Proximity to the Conducting Manikin at 1 GHz at the Chest Plane

Contour Presentation: A. Vertical B. Horizontal

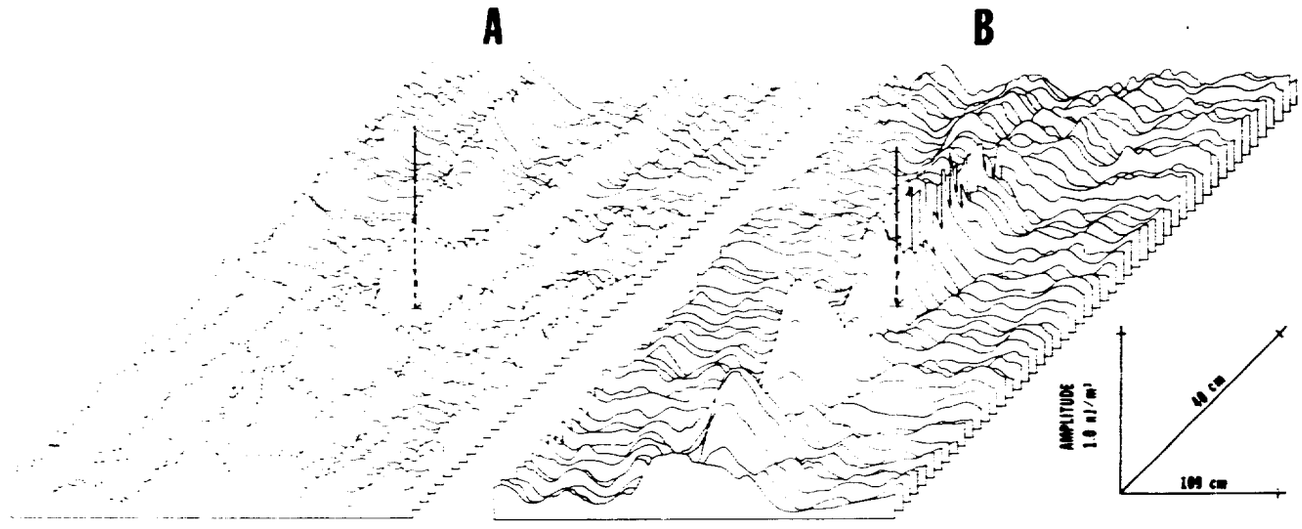

Figure 14

Energy Distribution in Proximity to the Conducting Manikin at 1 GHz at the Head Plane. 3-D Presentation:

A. Vertical B. Horizontal

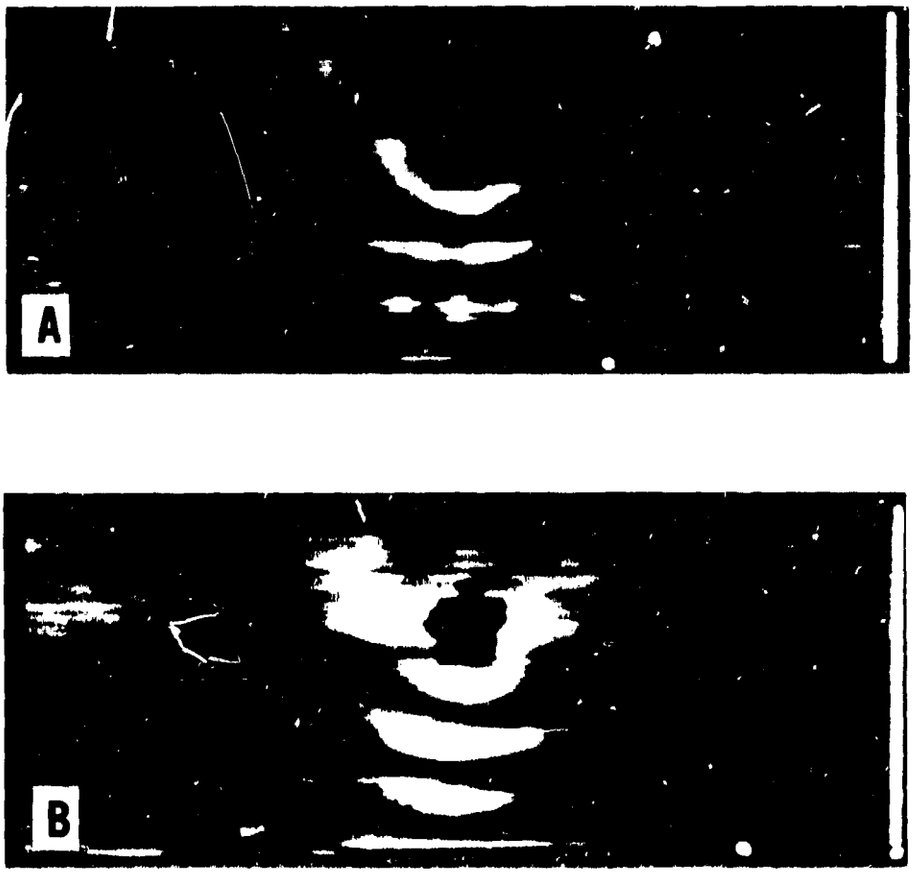

Figure 15

Energy Distribution in Proximity to the Conducting Manikin at 1 GHz at the Head Plane

Contour Presentation: A. Vertical B. Horizontal

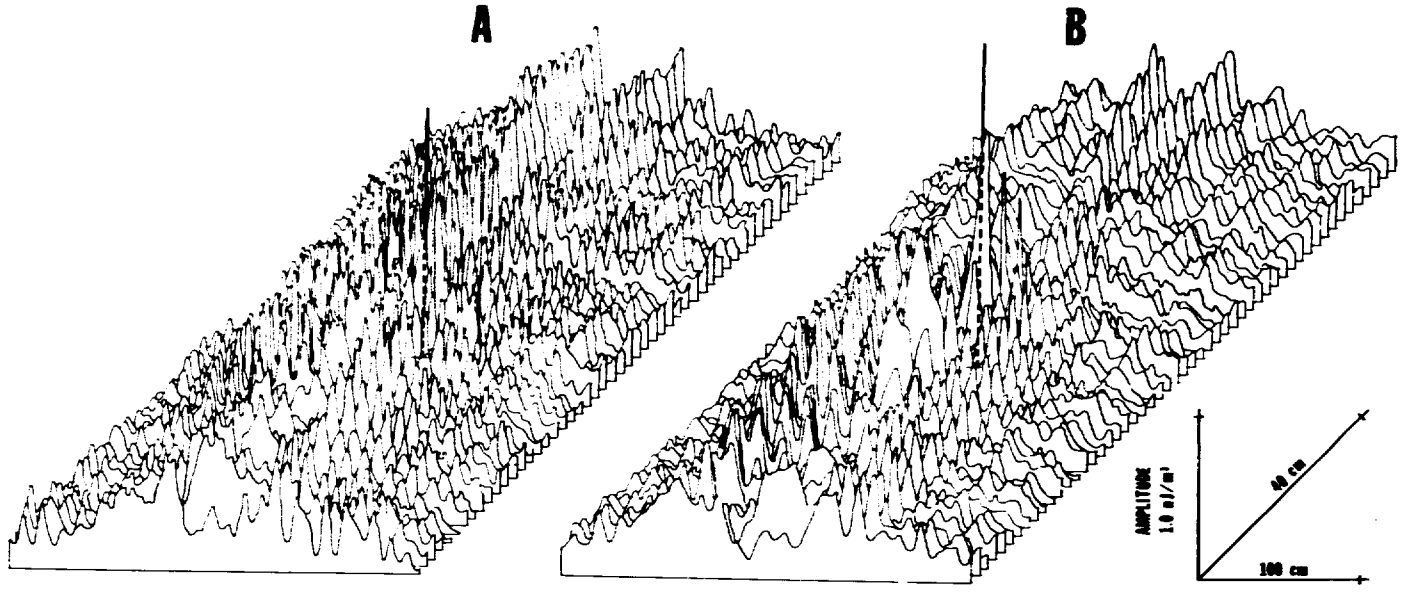

Figure 16

Energy Distribution in Proximity to the Conducting Manikin at 3 GHz at the Head Plane. 3-D Presentation:

A. Vertical B. Horizontal

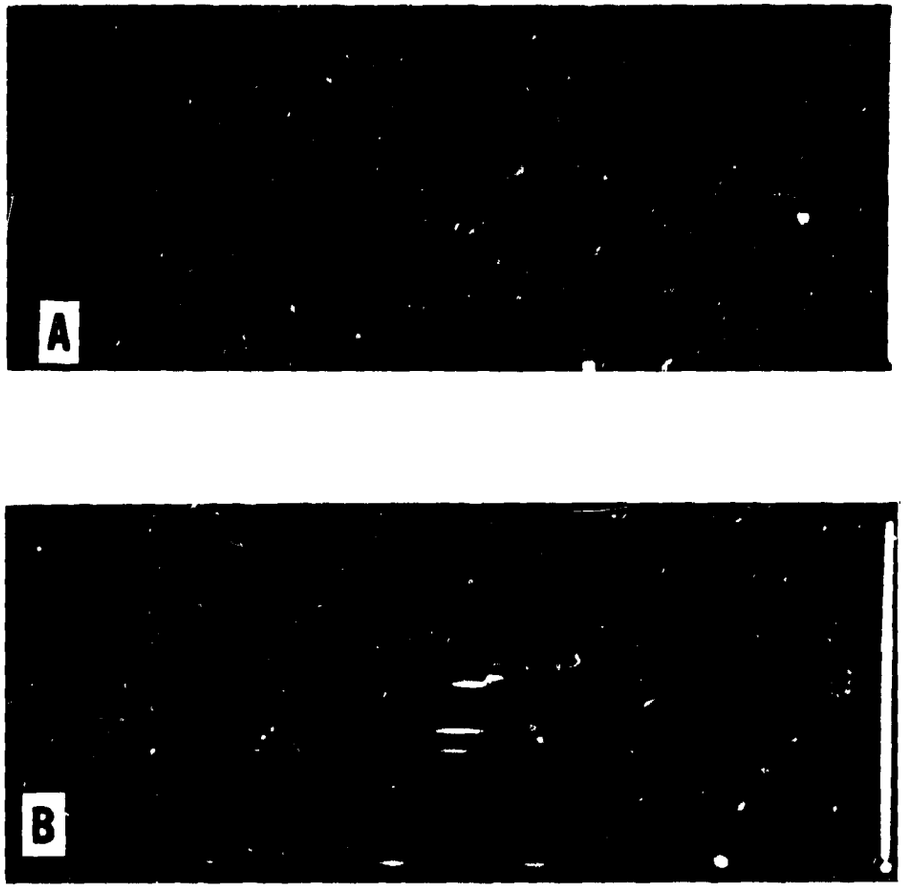

Figure 17

Energy Distribution in Proximity to the Conducting Manikin at 3 GHz at the Head Plane

Contour Presentation: A. Vertical B. Horizontal

Head Plane, 1 GHz. The results of comparable measurements made at 1 GHz at the head plane of the manikin are shown in Figures 14 and 15. The 3-D plots (Figure 14) are similar to those presented previously. The contour plots (Figure 15) were generated from the same data by using the computer output to intensity-modulate the beam of an oscilloscope, and the display was photographed. The range of the intensity scale in the photographs was adjusted to extend from white (field maximum) to black (field minimum). Since the scale in the computer plots was not calibrated, a qualitative overview of the diffraction field was obtained. Figures 14 and 15 show the parabolic nature of the fields, the standing waves, and the increased amplitude of the side structure when the incident wave was vertically polarized. Definite differences in the shadow area are related to the polarization of the field. The shadow is distinct with well-formed boundaries in the vertically polarized field (Figure 14), while it is almost nonexistent when the field is polarized horizontally. This suggests that considerable energy is reradiated from the nonilluminated side of the manikin's head, thus filling the shadowed area. A detailed theoretical discussion of a surface wave phenomenon that could explain this observation is found in King and Wu (8).

Head Plane, 3 GHz. Another series of measurements was made at 3 GHz at the head plane of the manikin (Figures 16 and 17). The most obvious effect of the change in frequency was the increase in complexity of the field patterns caused by changes in the spatial size of the variations. Although some of the information in the 3-D plots (Figure 16) is obscured, the standing wave peaks and the shadows can be identified. The parabolic pattern of the fields is most evident in the contour plots (Figure 17). Since the field structure is considerably more complex at this frequency, comparable plots would require a disproportionate amount of time and effort and be subject to a higher probability of error if produced manually. For this reason, computer-generated displays become more useful as the frequency increases. The amplitude of the structure at the sides of the field again appears generally lower when the radiation is horizontally polarized. However, the peak adjacent to the manikin is very high in amplitude and the amplitude of the ridges that form the boundaries of the shadow increases with distance from the manikin along the Z-axis (Figure 16 B).

The patterns of scattering from the manikin (Figures 12 through 17) suggest characteristic relationships between the wavelength of the incident radiation and the maximum transverse dimension (size) of the manikin at the plane of measurement. Table 1 summarizes the relationships for horizontally polarized radiation.

Since the field patterns at a given frequency and polarization incorporate expressions of the electrical properties, size and shape of the object, the manikin was deliberately made conductive to equate the electrical properties over the entire surface and to insure that all the incident energy was scattered, i.e., none was absorbed. Consequently, the pattern characteristics just described (Figures 12 through 17 and Table 1) were primarily related to the manikin's size and shape. The similarity in size and shape between the manikin and man makes it possible to compare the fields near the manikin with those in proximity to man. Since the influence of size and shape on the patterns was nearly equal, any differences should be related to the energy absorbed by the man.

Table 1

Field Pattern Characteristics in Proximity to Conducting Manikin Illuminated by Horizontally Polarized Wave

Frequency (GHz)	Wavelength (cm)	Measurement Plane	Size (cm)	Ratio of Size to Wavelength	Relative Amplitude of Adjacent Peak	Relative Amplitude of Shadow Boundaries	Energy in Shadow
1	30	Chest	49.7	1.7	very high	increases	minimal
3	10	Head	14.8	1.5	very high	increases	minimal
1	30	Head	14.8	0.5	medium	decreases	sufficient to obscure shadow

Man

The characteristic reflection and diffraction patterns in proximity to man are shown in Figures 18 through 24.

Chest Plane, 1 GHz. Figures 18 and 19 show the energy distribution as a function of polarization at 1 GHz on a plane at chest level. A gross comparison of the field patterns in proximity to man, the manikin and the cylinder indicates certain general characteristics that are held in common. Standing waves appear on the illuminated side of man and a shadowed region is produced on the side opposite the antenna (Figure 18). The parabolic structure of the field and reduction in amplitude of the side structure due to polarization is shown in the contour plots (Figure 19).

Figure 20 is a computer-generated, contour display of the same data used to manually construct Figure 19 A and is included to provide perspective and a direct comparison of the two methods of data presentation. The same field characteristics appear in both types of contour plots.

A more detailed comparison of the energy distribution on a plane at the level of the chest in man (Figure 18) with that on the same plane near the manikin (Figure 12) and near the cylinder (Figure 9) indicates differences that are apparently dependent on differential absorption by the man. The peaks in the standing waves diminish in amplitude with distance from both the manikin and the cylinder. If man is the test object, however, the peaks are lower in initial amplitude but remain nearly constant with distance. The characteristic reduced amplitude of the standing wave peaks, and of the peak adjacent to the man in particular, suggests absorption of the energy by the human subject.

Head Plane, 1 GHz. The field distribution at 1 GHz around the head of the man is shown in Figures 21 and 22. Comparison of this distribution with the patterns near the head of the manikin at the same polarization demonstrates a definite reduction in the amount of energy scattered by the man (Figures 14 and 21). Since the incident energy is the same in both cases, the reduction is strong evidence of absorption. Another difference in the patterns is found in the shadow area when the incident wave is horizontally polarized. The shadow region on the nonilluminated side of the man's head contains minimal electrical energy (B in Figures 21 and 22) while a significant amount is present in the analogous area near the manikin (B in Figures 14 and 15). This suggests that the surface currents generated on the manikin and the consequent radiated energy are not present to the same degree on man because of the reduced conductivity of the man.

Head Plane, 3 GHz. Figures 23 and 24 indicate the field patterns at 3 GHz on a plane at the level of the man's head. The pattern of electric energy distribution is generally similar to that near the head of the manikin at the same frequency, as is particularly evident in comparing the corresponding contour plots (A in Figures 17 and 24 and B in Figures 17 and 24, respectively).

Although the patterns of energy distribution are similar around the man and the manikin under all conditions studied, there are definite differences in the amplitude of the

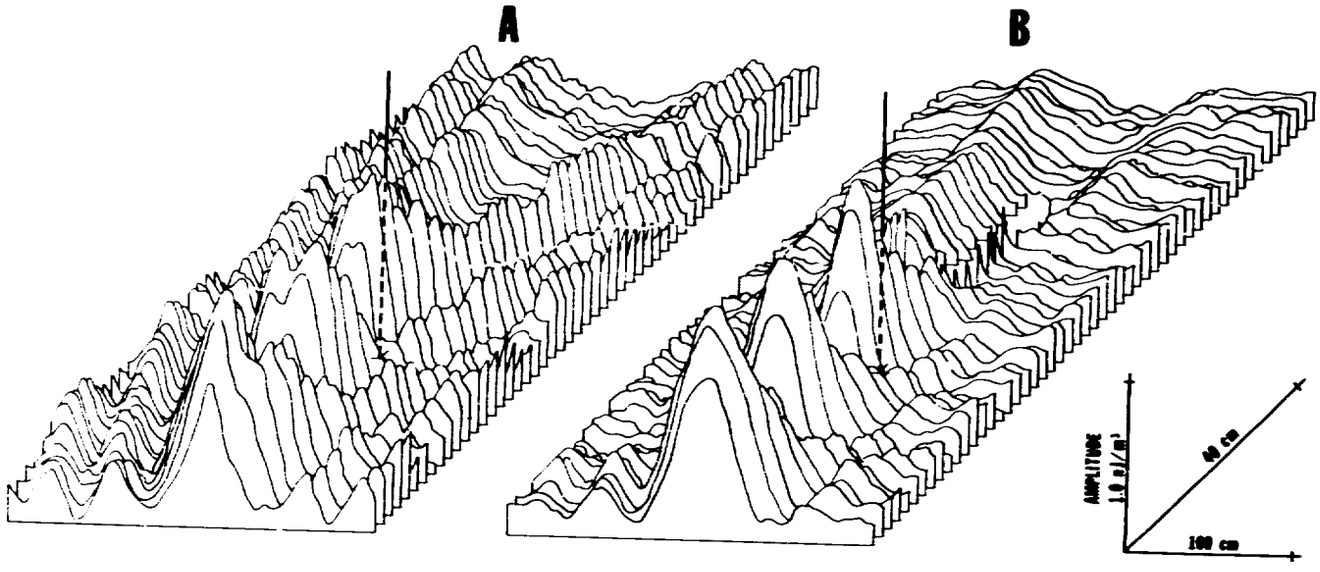

Figure 18

Energy Distribution in Proximity to Man at 1 GHz at the Chest Plane. 3-D Presentation:

A. Vertical B. Horizontal

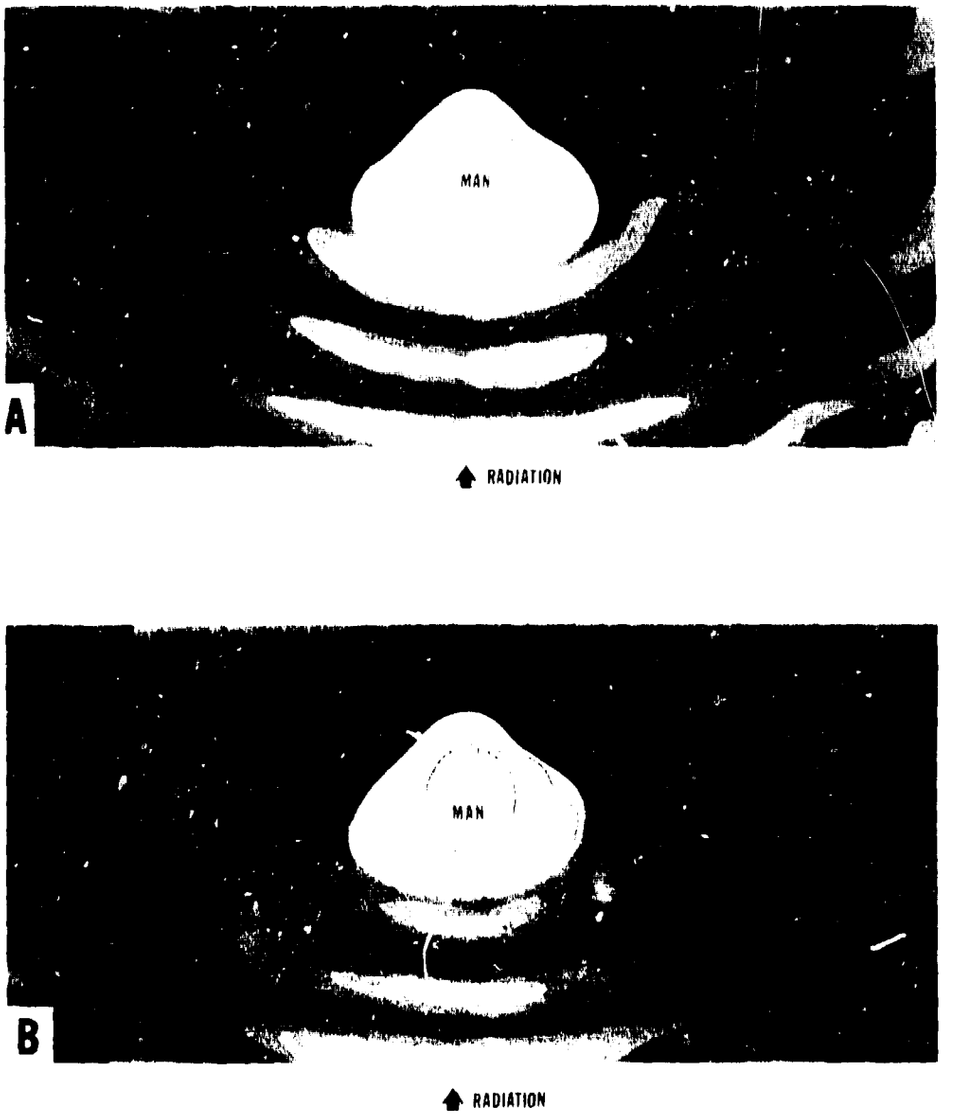

Figure 19

Energy Distribution in Proximity to Man at 1 GHz at the Chest Plane

Contour Presentation: A. Vertical B. Horizontal

Figure 20

Computer-Generated Contour Presentation of the Data used to Construct the Manual Contour Plot in Figure 19 A

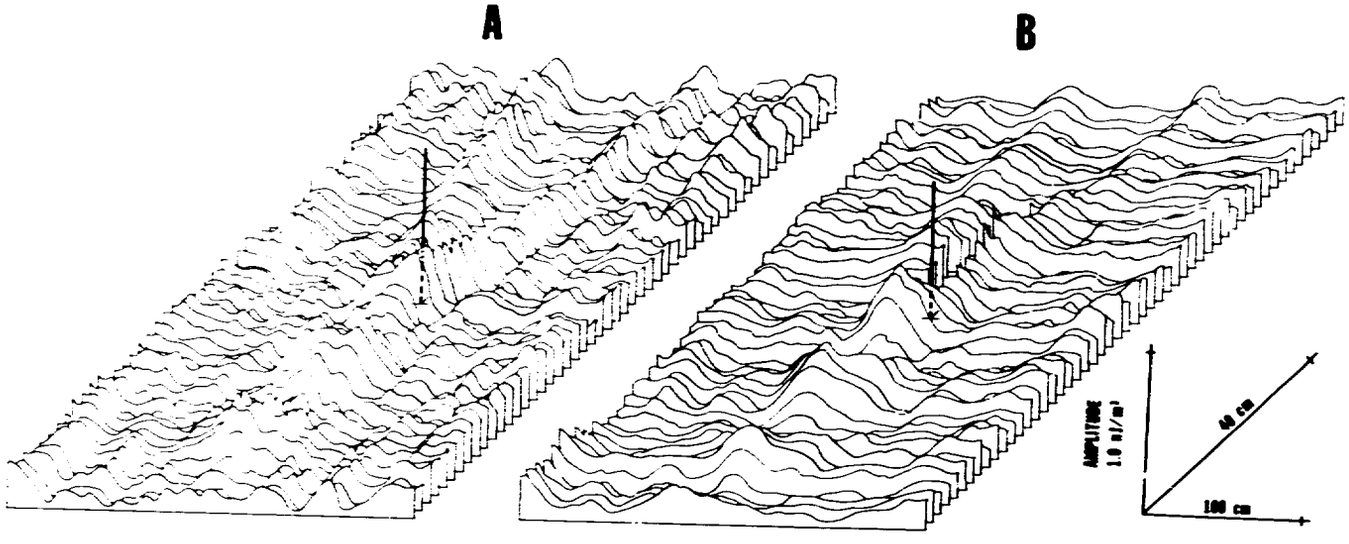

Figure 21

Energy Distribution in Proximity to Man at 1 GHz at the Head Plane. 3-D Presentation:

A. Vertical B. Horizontal

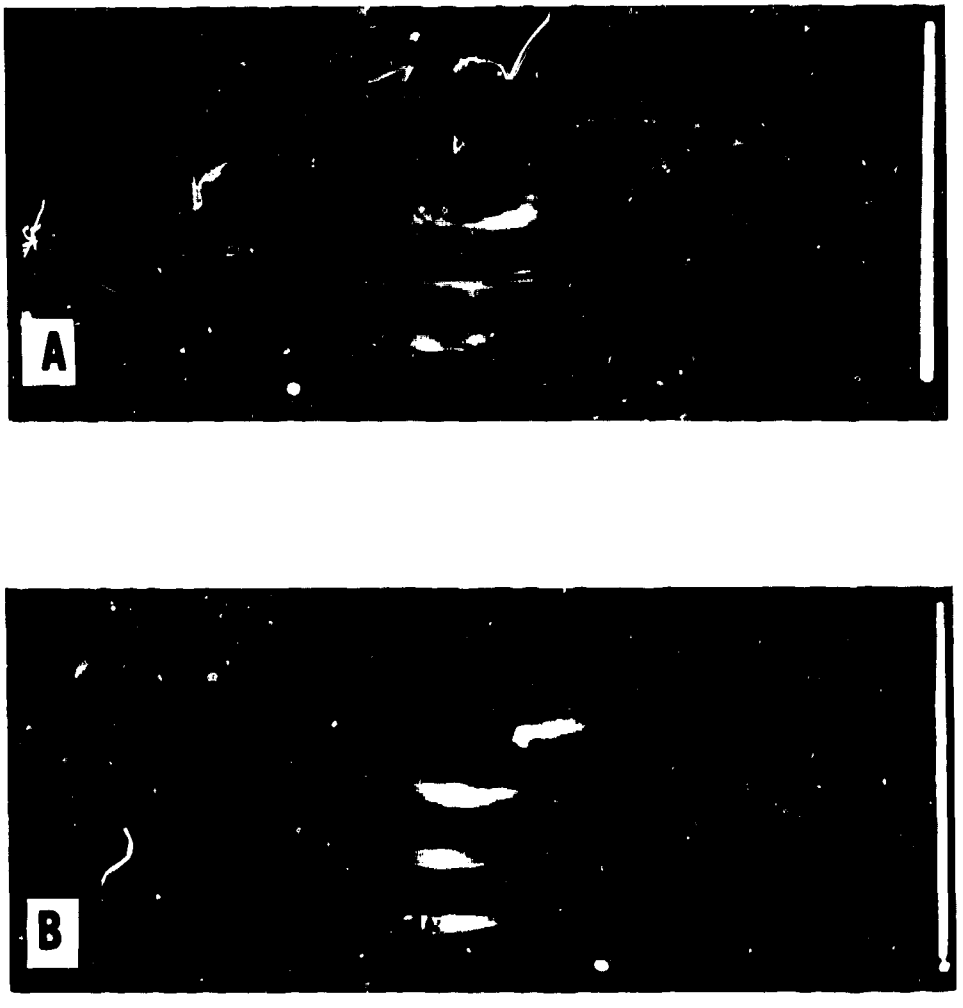

Figure 22

Energy Distribution in Proximity to Man at 1 GHz at the Head Plane

Contour Presentation: A. Vertical B. Horizontal

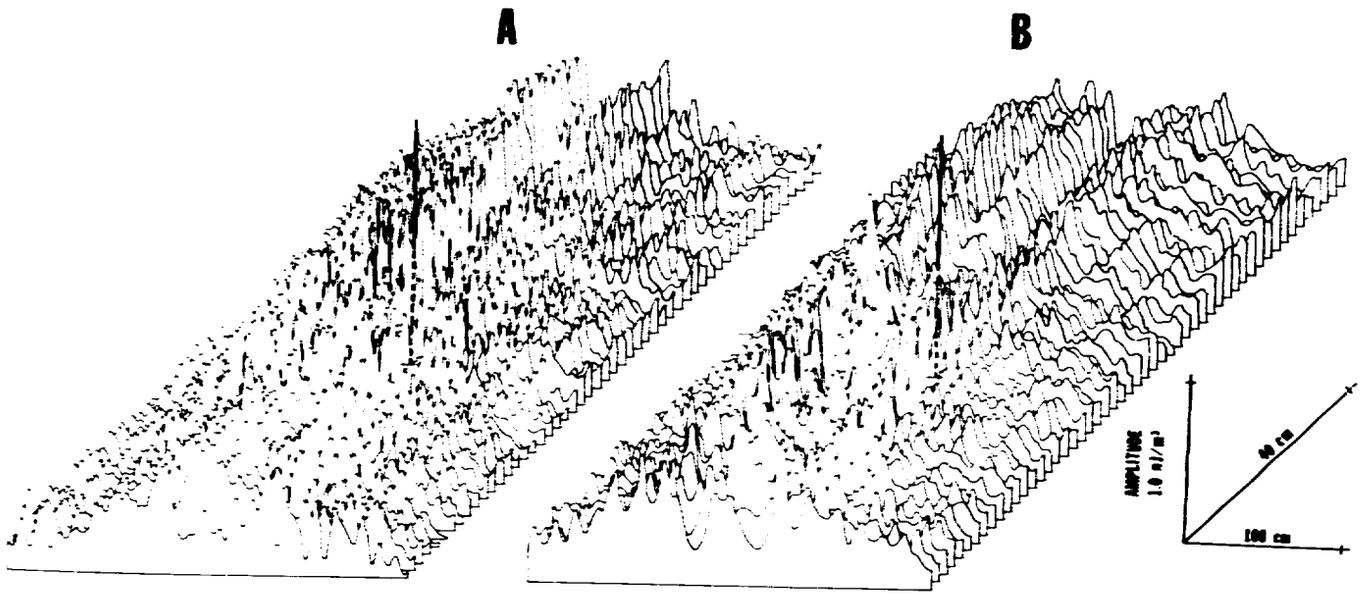

Figure 23

Energy Distribution in Proximity to Man at 3 GHz at the Head Plane. 3-D Presentation:

A. Vertical B. Horizontal

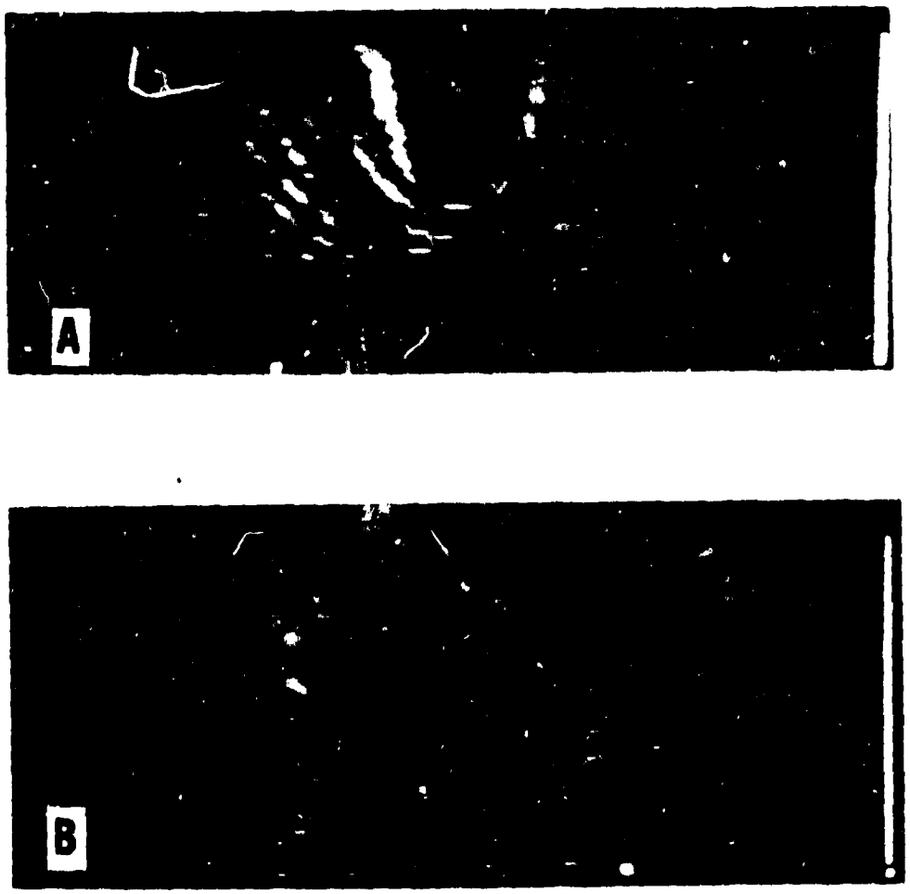

Figure 24

Energy Distribution in Proximity to Man at 3 GHz at the Head Plane

Contour Presentation: A. Vertical B. Horizontal

scattered energy. This is especially evident in comparing the standing-wave peaks near the man (B in Figures 18, 21, and 23) with the analogous peaks near the manikin (B in Figures 12, 14, and 16). The effect of the ratio of object size to wavelength on the energy distribution was demonstrated for the manikin (Table 1). The ratio apparently does not have the same effect on the distribution if man is illuminated under the same conditions.

PHASE RELATIONSHIPS

A determinant of the E-field amplitude measured at any given point in space near a scattering object is the phase relationship between the field incident on the object and that reflected from it. Absorption estimations based on determinations of the difference in amplitude between the incident and reflected energy could, therefore, be in error if these relationships are not considered. The necessary phase information is inherent to the E-field patterns previously described. It should be recalled that in a standing wave, the maxima and minima in resultant field amplitudes occur where the incident and reflected waves are in and out of phase, respectively. It is known that the position of the minimum in a standing wave can be located with greater accuracy than that of a maximum (6), however, the incident wave must be sufficiently high in amplitude to insure that the amplitude minima will be well above the noise level of the detector. In the context of the present measurements, this implies that the field incident on the man would be relatively high in intensity. Essentially the same information can be gained by location of the field maxima with the advantage that the incident field can be reduced in intensity; therefore, this approach was adopted for the present study.

Figure 25 depicts the E-field maxima calculated by King and Wu (8) for a conducting cylinder illuminated by a vertically polarized plane wave. The E-field maxima measured on a plane at chest level around the cylinder, manikin and man are superimposed on the theoretical curves. The parabolic structure of the curves is immediately apparent. The reference point common to all the test objects is located at the tip of the arrow labeled "incident beam." Dependent on the elevation of the measurement plane, this reference lies at some point on the vertical line in the 3-D plots.

Figure 25 shows the relationship between the theoretical distribution of in-phase components predicted for the cylinder and that actually measured in the present experiments. The 30-cm diameter of the cylinder used in the study at 1 GHz provides a direct comparison of the experimental results with the theoretical treatment, since the ratio of diameter to wavelength in both cases was 1. The agreement between the curves provides assurance that the cylinder can be used under the existing conditions as a calibrating device as well as a connecting link to relate the fields in proximity to the man and manikin to those associated with simpler, better-understood objects described in the literature. The correlation between the curves also implies that the field is relatively planar since the theoretical distribution assumed a plane wave.

Equiphase lines are also constructed along the E-field maxima generated by the man and manikin under the same exposure conditions. The agreement between this pair of curves is very good. Since the dielectric properties of the man and manikin are different,

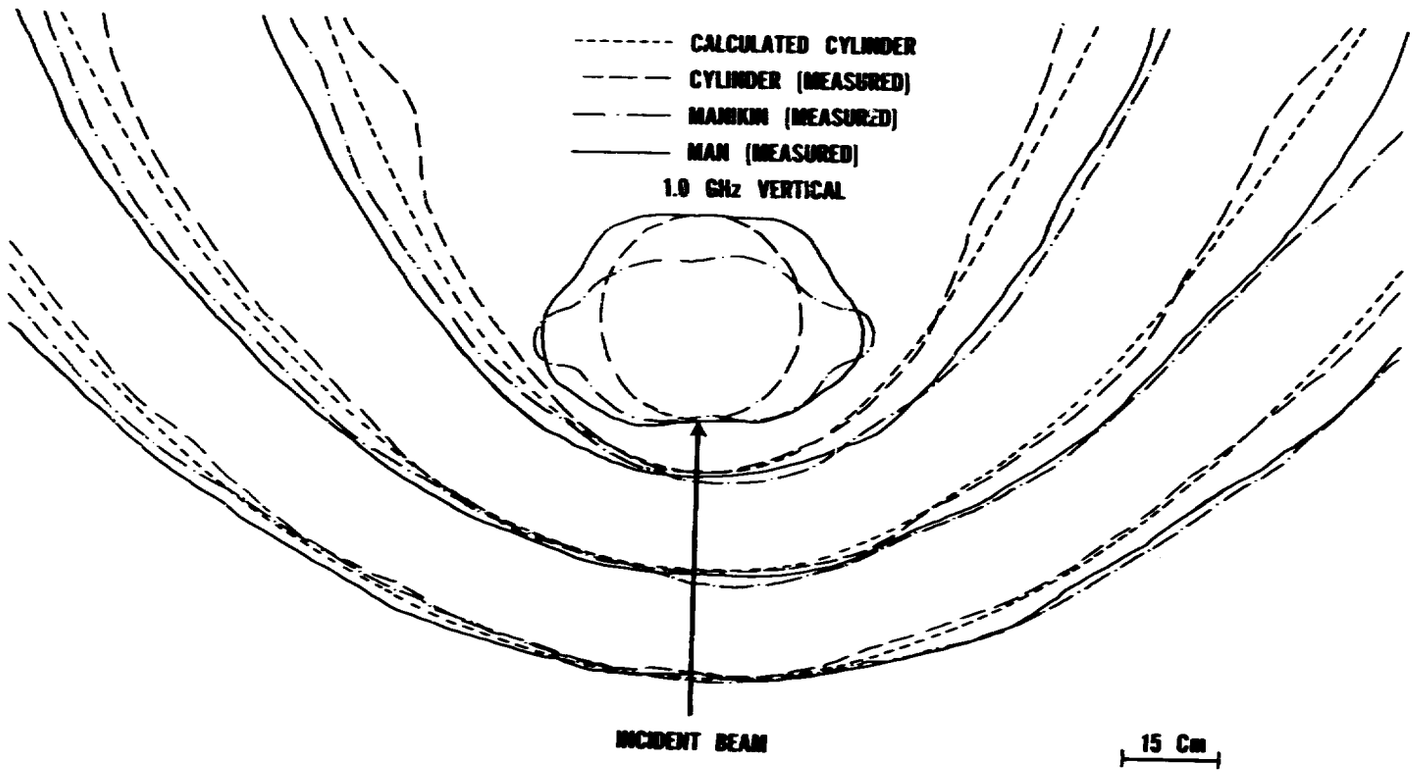

Figure 25

Electric Field Maxima Near Diffracting Objects

it appears that the phase distribution is not dependent on these properties. On the other hand, the pair of curves for the man and manikin do not generally coincide with those for the measured and calculated cylinder. Since the cylinder and the manikin are both conductive, this suggests that it is the size of the man or other object, rather than his electrical properties, that determines the phase distribution of the fields in his vicinity.

The equiphase lines from each of the objects intersect a line that is normal to both the advancing wavefront and the illuminated surface of the object. The relationship between the wavelength of the radiation and the energy distribution patterns is most clearly evident on this normal where the intersections occur at odd multiples of a quarter wavelength from the reflecting object. It is apparent in the preceding figures that the standing wave maxima or peaks occur at these intersections.

For maximum utility and accuracy, an estimation of absorbed energy based on external field measurements should not be critically dependent on small differences in size such as those normally present in a population. Figure 25 indicates that phase conditions are independent of the size of the reflecting object only on the normal for the objects used in the present experiments. Since the phase relationships at any point other than on the normal are dependent on the size, and the amplitude at a given point is dependent in part on the phase conditions, a correction for phase effects due to the size of the object is required if the measurement is taken at any point in the field other than on the normal.

CONCLUSIONS

A series of studies of the energy distribution in proximity to man during microwave illumination is in progress. The studies indicate several concepts that are important to investigations of the bioeffects of nonionizing radiation. A pronounced diffraction field is generated in space in proximity to man during illumination by microwave energy. The characteristics of the field are dependent on the complex relationships between the frequency and polarization of the radiation and the geometry and dielectric properties of the man. The effects of each of these parameters on the diffraction field can be isolated and identified, and the field characteristics can be compared to data obtained from both theoretical and experimental studies of objects having less complex shape and composition.

Definite standing waves are formed on the illuminated side of man and pronounced areas of shadow appear on the opposite side. Considerable energy is also present in the field alongside man, if the electric vector of the incident wave is parallel to the long axis of the man. If the wave is polarized horizontally relative to the man, this energy is redistributed so that the amount present at the lateral aspects is much reduced. Under all of the conditions tested, a considerable amount of the energy incident on the man was reflected. Field intensities in his vicinity may, therefore, vary over a very wide range.

Power measurements in proximity to man for safety monitoring may be subject to gross errors in interpretation if diffraction fields are not taken into consideration. This is particularly true at higher frequencies where a small change in position of the measuring device could result in large differences in the magnitude of the measured field intensity. Similar errors in interpretation could result if the diffraction fields of other nearby

personnel or reflecting objects are not taken into account. The same considerations place constraints on the experimental design of bioeffect studies.

Probably the most significant of the benefits that may ultimately accrue from this new experimental approach is the potential development of a noninvasive method of estimating the energy absorbed from a microwave field by man and other living organisms. The characterization of the effect of each of the factors contributing to the diffraction field forms the foundation for such a method.

A unique advantage of the approach is that both the complex dielectric properties and the geometry of man are automatically taken into account in the proper perspective. The risk of error concomitant with extrapolations from animal models or from even simpler static models is therefore minimized or obviated. A judicious combination of high sensor sensitivity, low incident field intensity and short period of exposure provides the information with minimum exposure of the subject.

Direct measurement of the diffraction fields in proximity to man will provide information concerning his interaction with a microwave environment that can be obtained in no other way.

REFERENCES

1. Adey, A. W., Scattering of microwaves by long dielectric cylinders. Wireless Engineer, 33:259-264, 1956.

2. Bassett, H. L., Ecker, H. A., Johnson, R. C., and Sheppard, A. P., New techniques for implementing microwave biological-exposure systems. IEEE Transactions on Microwave Theory and Techniques, MTT 19:197-204, 1971.

3. Beischer, D. E., and Reno, V. R., Microwave reflection and diffraction by man. Proceedings of the International Symposium on Biologic Effects and Health Hazards of Microwave Radiation. Warsaw, Poland, 1973. (In press).

4. Beischer, D. E., and Reno, V. R., Microwave energy distribution measurements in proximity to man and their practical application. Conference on the Biological Effects of Nonionizing Radiation. New York: Annals of New York Academy of Sciences, 1974. (In press).

5. Crispin, J. W., Jr., and Siegel, K. M., Methods of Radar Cross-Section Analysis. New York: Academic Press, 1968.

6. Giordano, A. B., Measurement of standing wave ratio. In M. Sucher and J. Fox (Eds.), Handbook of Microwave Measurements. New York: Polytechnic Press, 1963. Pp. 73-133.

7. Harvey, A. F., Measurements on and properties of materials. In A. F. Harvey, Microwave Engineering. New York: Academic Press, 1963. Pp. 233-279.

8. King, R. W. P., and Wu, T. T., The Scattering and Diffraction of Waves. Cambridge, Mass.: Harvard University Press, 1959.

9. Reno, V. R., and Beischer, D. E., Microwave reflection, diffraction and transmission by man: A pilot study. NAMRL-1183. Pensacola, Fla.: Naval Aerospace Medical Research Laboratory, 1973.

10. Ruch, T. C., and Fulton, J. F. (Eds.), Medical Physiology and Biophysics. Philadelphia: W. B. Saunders Co., 1961. Pp. 752-770.

11. Silver, S., Parabcloidal reflectors. In S. Silver (Ed.), Microwave Antenna Theory and Design. Boston: Boston Technical Publishers, 1964. Pp. 415-464.

12. Tang, C. C. H., Backscattering from dielectric-coated infinite cylindrical obstacles. Journal of Applied Physiology, 28:628-633, 1957.

13. Tell, R. A., Microwave energy absorption in tissue. Technical Report. Rockville, Md.: Environmental Protection Agency, Twinbrook Research Laboratory. National Technical Information Service No. PB 208 233, 1972.

14. Tinga, W. R., and Nelson, S. O., Dielectric properties of materials for microwave processing-tabulated. Journal of Microwave Power, 8:23-65, 1973.

15. Wacker, P. F., and Bowman, R. R., Quantifying hazardous electromagnetic fields: Scientific basis and practical considerations. IEEE Transactions on Microwave Theory and Techniques, MTT 19:178-187, 1971.